

Evaluation of Orbiter Performance and Nose Heating at Mach 3.8

February 26, 2020

1 Introduction

1.1 3-D orbiter shape

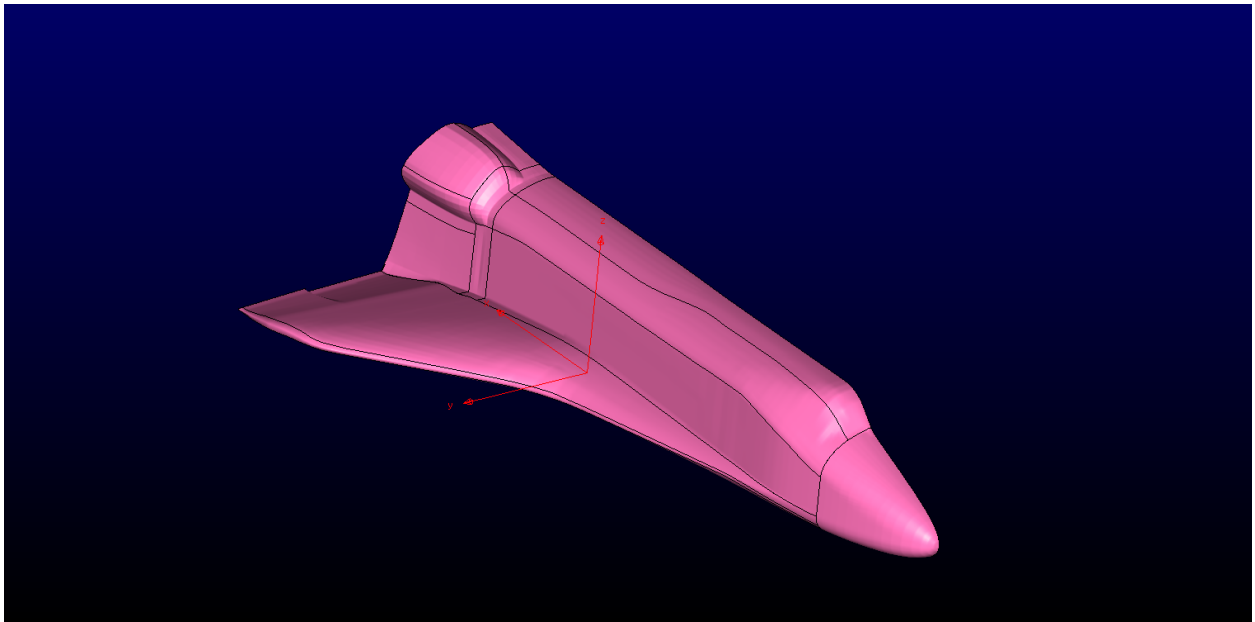


Figure 1: 3-D orbiter

1.2 Data from published literature

The equations used to plot the data in figure 2 were from [2]

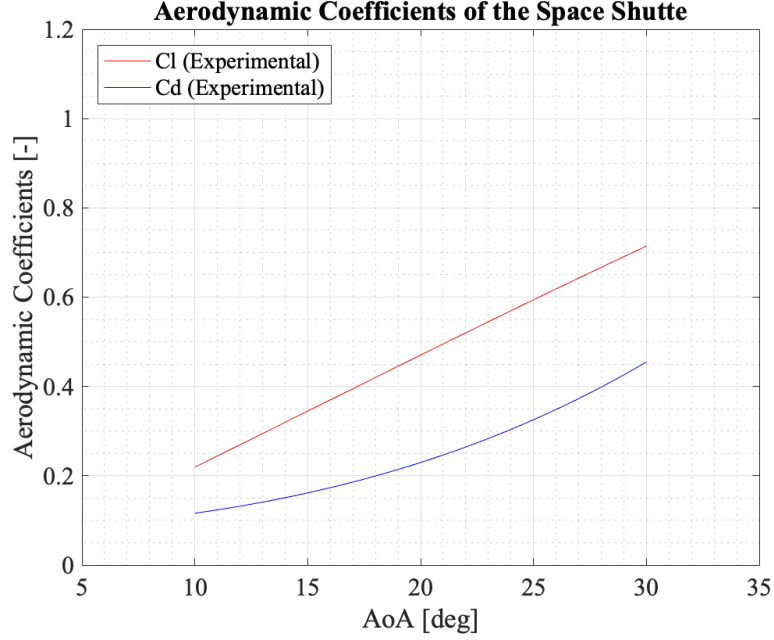


Figure 2: Experimental models and predictions of C_L & C_D

Table 1: Freestream conditions and expected stagnation conditions at wing/nose LE

Mach number	3.8
Post-shock mach number	0.4407
Pressure p^1	1090.16 Pa
Temperature T	227.13 K
Density ρ	$0.0167 \text{ kg} \cdot \text{m}^{-3}$
p_2/p_1 at M=3.8	16.68
T_2/T_1 at M=3.8	3.743
Isentropic p_o/p at M=0.44	1.142
Isentropic T_o/T at M=0.44	1.035
Stagnation pressure	20765.98 Pa ($p \cdot p_2/p_1 \cdot p_o/p$)
Stagnation temperature	883.303 K ($T \cdot T_2/T_1 \cdot T_o/T$)

p, T, ρ : at 100,000 ft from 1976 Digital Dutch Standard Atmospheric Calculator

(URL: <https://www.digitaldutch.com/atmoscalc/>)

Isentropic relations and pressure/temp discontinuity across shock: From appendix A of Modern Compressible Flow by J.D. Anderson [1].

2 Methodology

2.1 Shots of the Orbiter grid

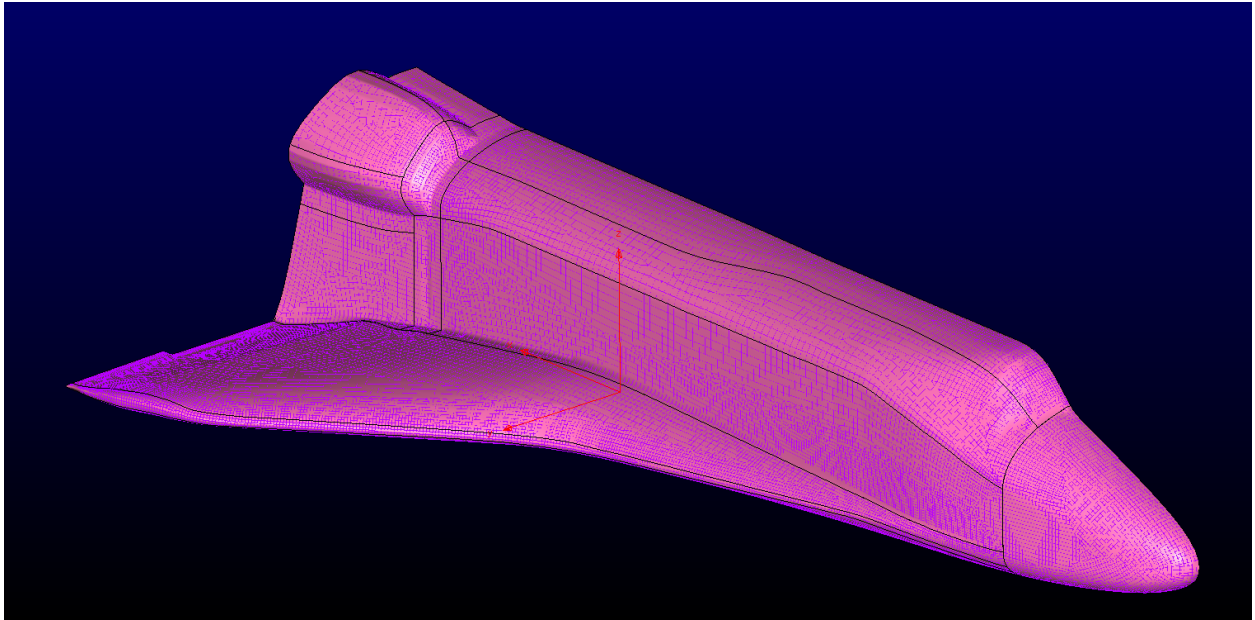


Figure 3: Entire grid of the orbiter

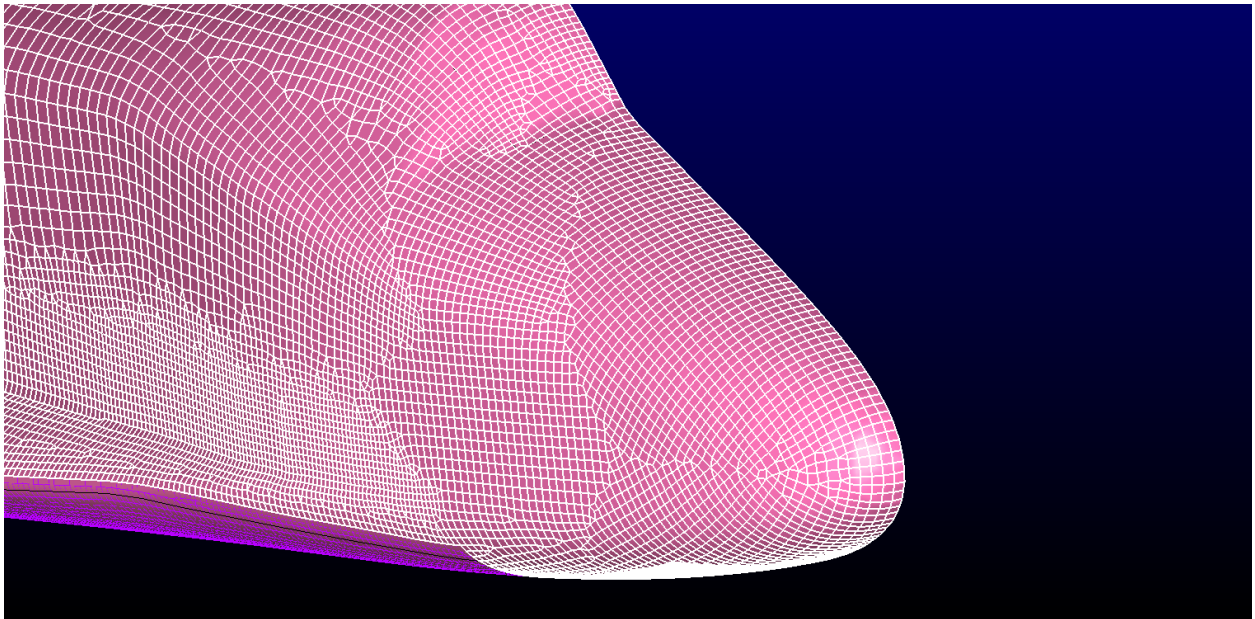


Figure 4: Nose of the orbiter

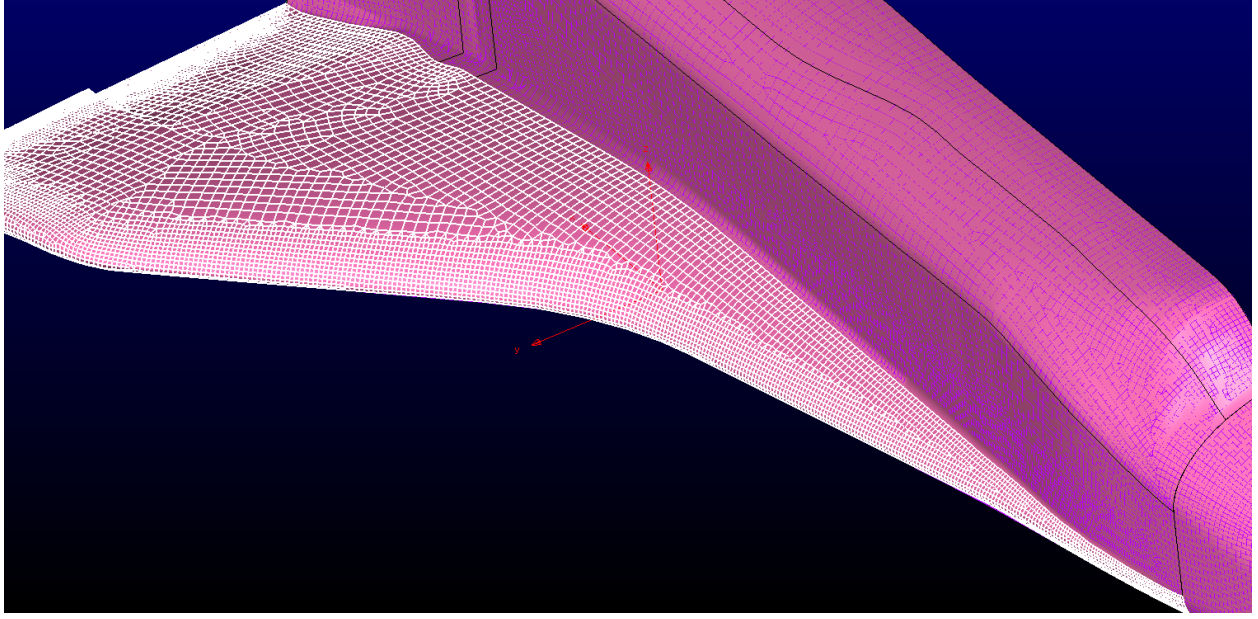


Figure 5: Midspan of the wing of the orbiter

2.2 Fluent setup

Table 2: General grid information

Cell count	1,375,480 Cells
Min/max included angles	max: 179.844 deg min: 0.06222 deg
Normal-to-wall spacing	$\Delta s = 0.001$
Boundary conditions	Inlet/hemispherical shell: pressure far-field Outlet/back of hemispherical shell: pressure outlet Orbiter surface (including backside): wall Plane of Symmetry: symmetry
Reference values	Area: 257.47 [m ²] Density: 1.672e-2 [kgm ⁻³] Enthalpy: 8.907e+5 [Jkg ⁻³] Length: 38.424 [m] Gauge pressure: 0 [Pa] Temperature: 227.13 [K] Velocity: 1147.86 [m/s] Viscosity: 1.789e-05 [kgm ⁻¹ s ⁻¹] Ratio of specific heat: 1.4
Submodels	Numerical Scheme: Implicit AUSM
Method and Accuracy	Gradient: least-squares cell based Flow: first order upwind

3 Results

3.1 Proof of convergence history

Please see Appendix

3.2 Table of final lift and drag coefficients and related forces

Case	C_L [-]	C_D [-]
10	0.143	0.075
20	0.341	0.174
30	0.545	0.371
Adapted 20	0.342	0.173

3.3 Plot of lift and drag and L/D vs. AOA with peak L/D identified

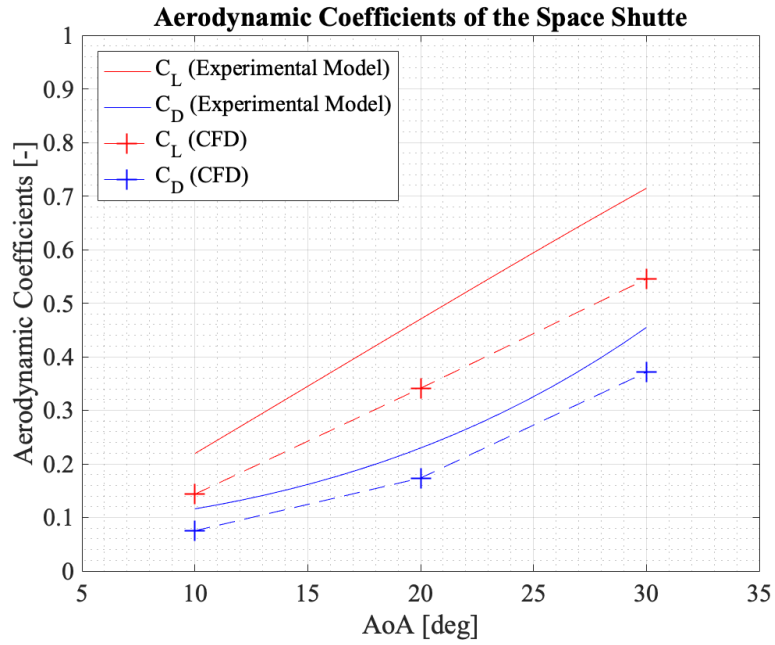


Figure 6: Comparison of the C_L and C_D results from the experimental model and the CFD cases ran

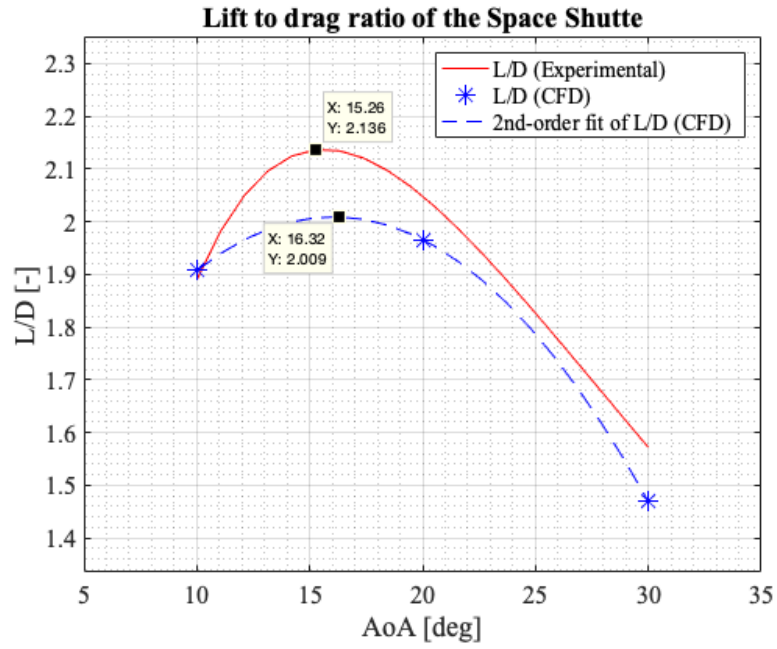


Figure 7: Comparison of the lift-to-drag ratios from the experimental model and the CFD cases ran

3.4 Pressure and temperature contours with streamlines

3.4.1 AoA = 10°

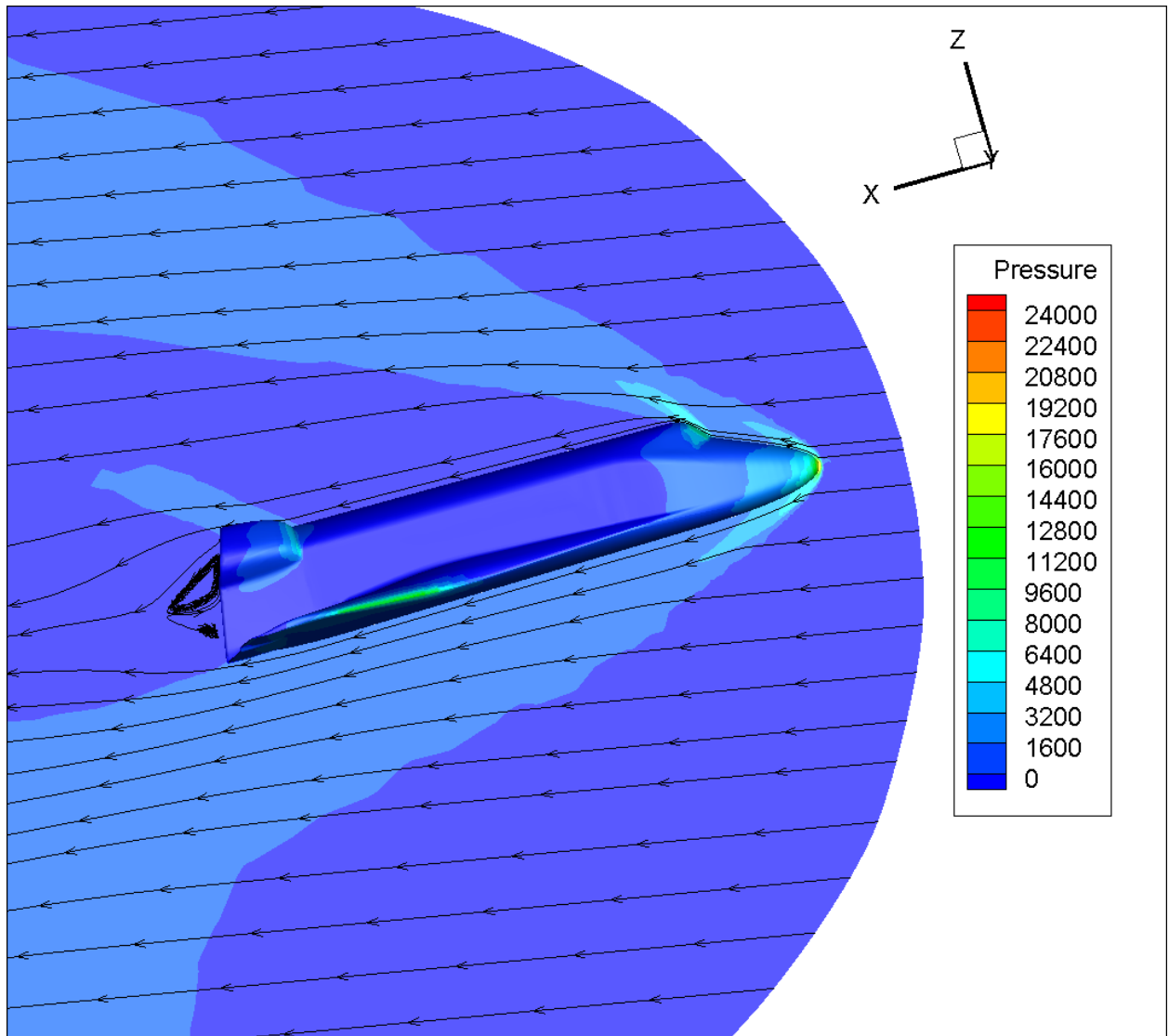


Figure 8: Pressure contour at the symmetry plane of the orbiter at 10 degs AoA

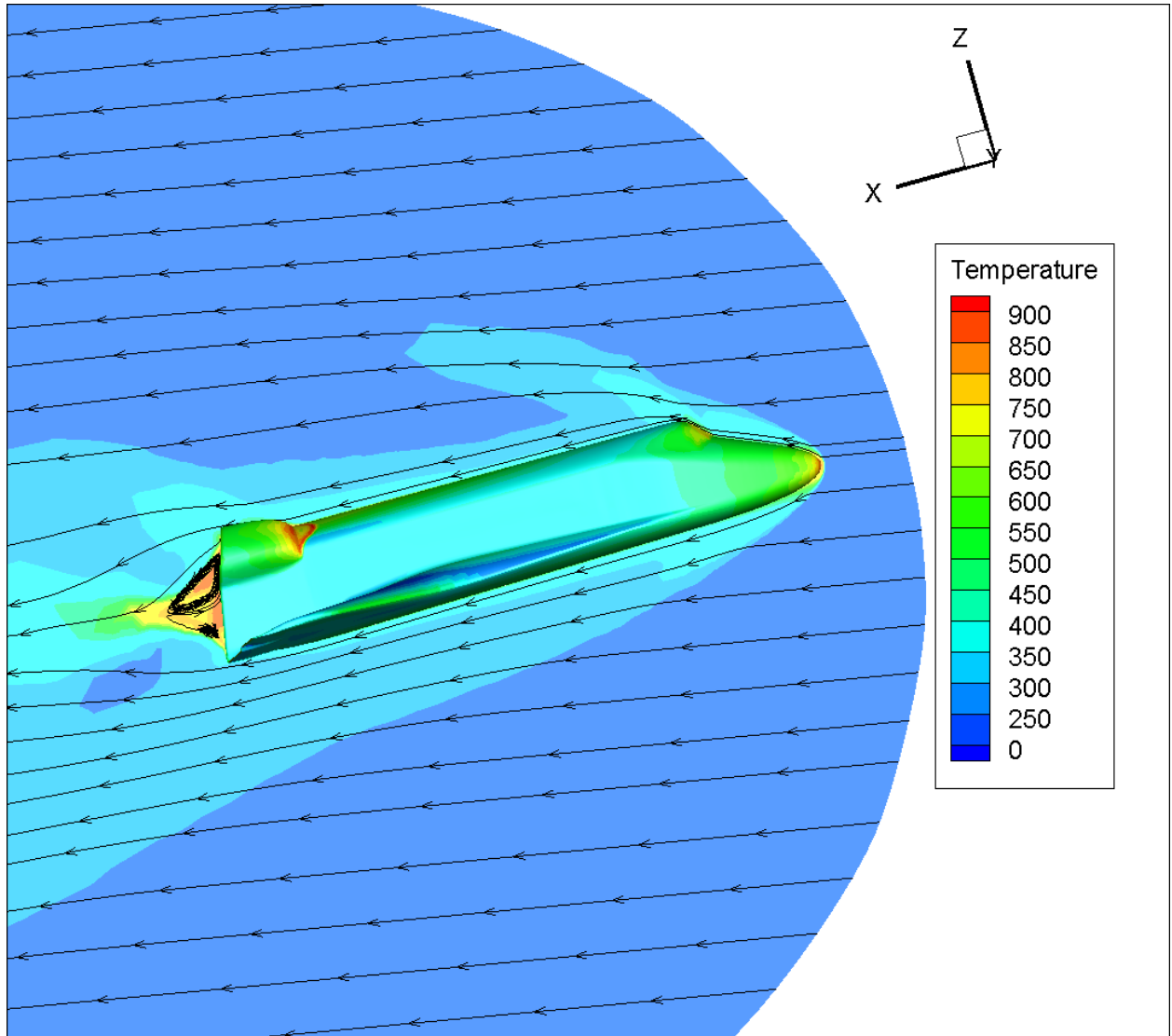


Figure 9: Temperature contour at the symmetry plane of the orbiter at 10 degs AoA

3.4.2 AoA = 20°

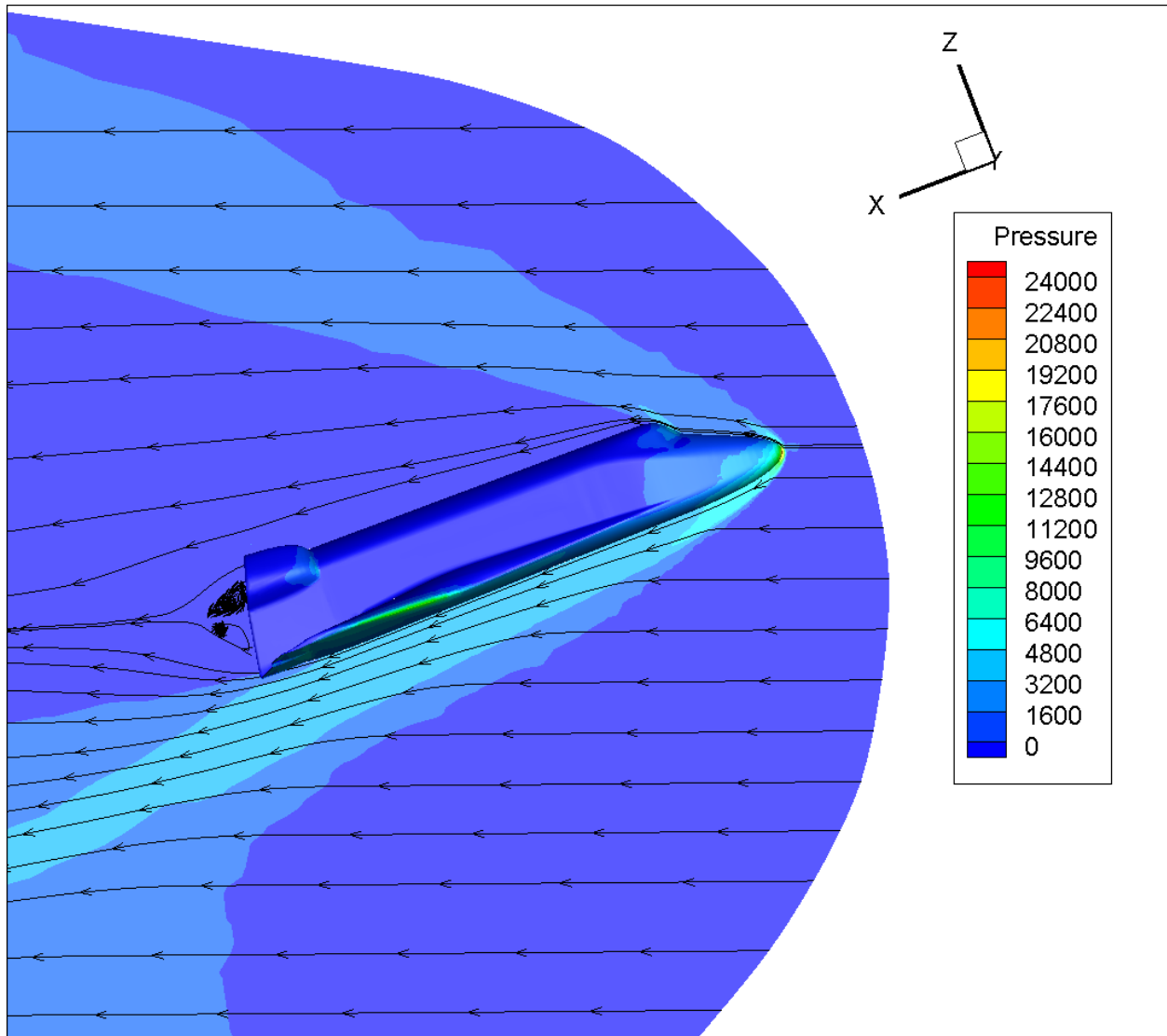


Figure 10: Pressure contour at the symmetry plane of the orbiter at 20 degs AoA

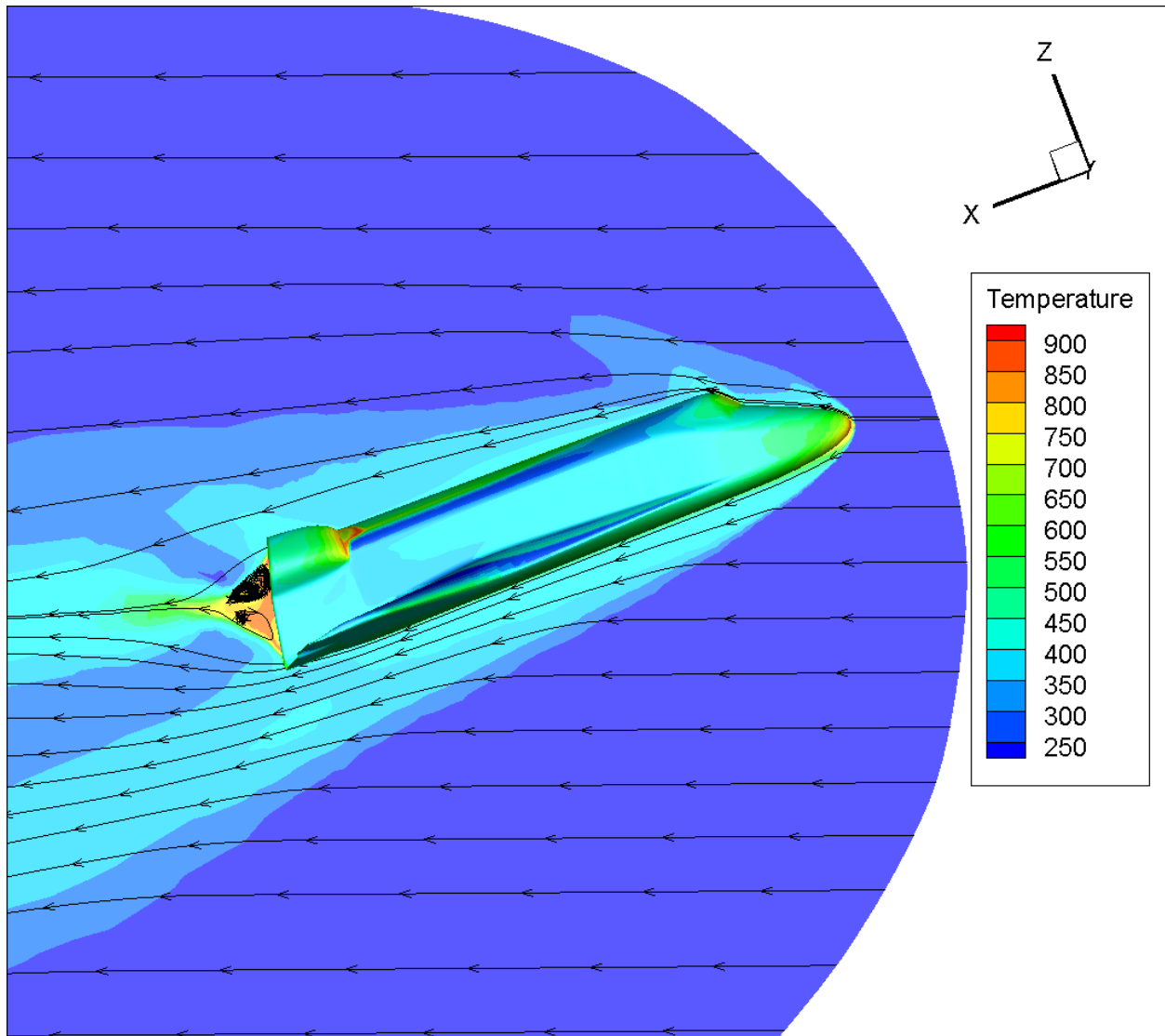


Figure 11: Temperature contour at the symmetry plane of the orbiter at 20 degs AoA

3.5 Results of grid adaptation

3.5.1 Side by side of contour plots

3.5.2 Side by side of mesh

3.5.3 Table of force coefficients

3.5.4 Fluent settings used to adapt grid

Appendix

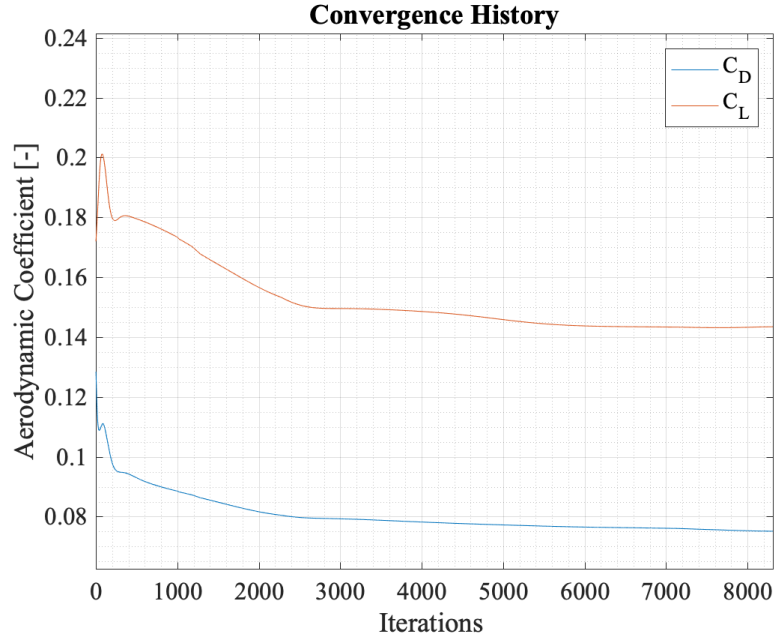


Figure 12: Convergence history for $\text{AoA} = 10^\circ$

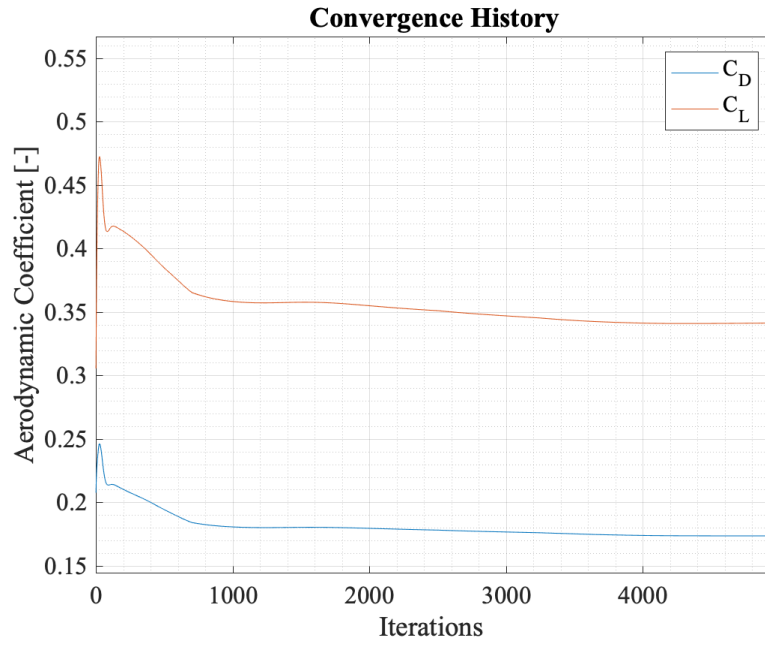


Figure 13: Convergence history for $\text{AoA} = 20^\circ$

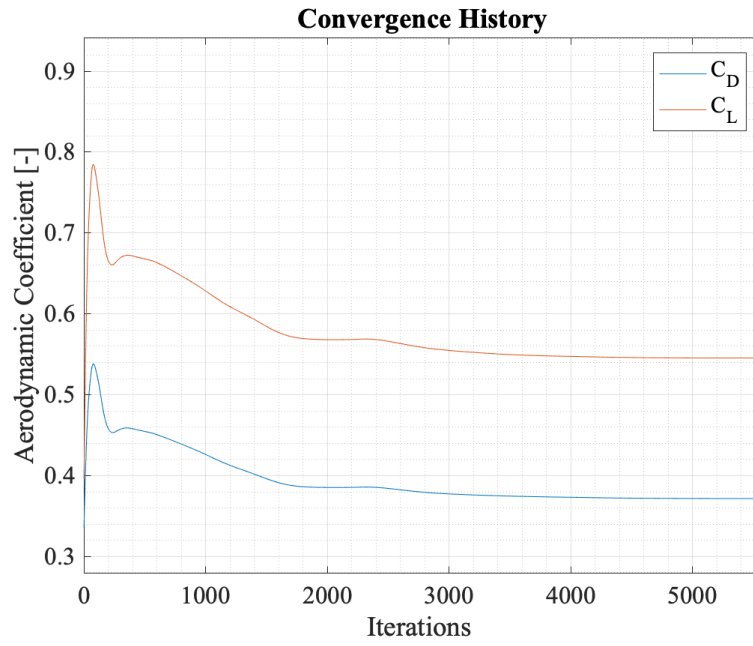


Figure 14: Convergence history for $\text{AoA} = 30^\circ$

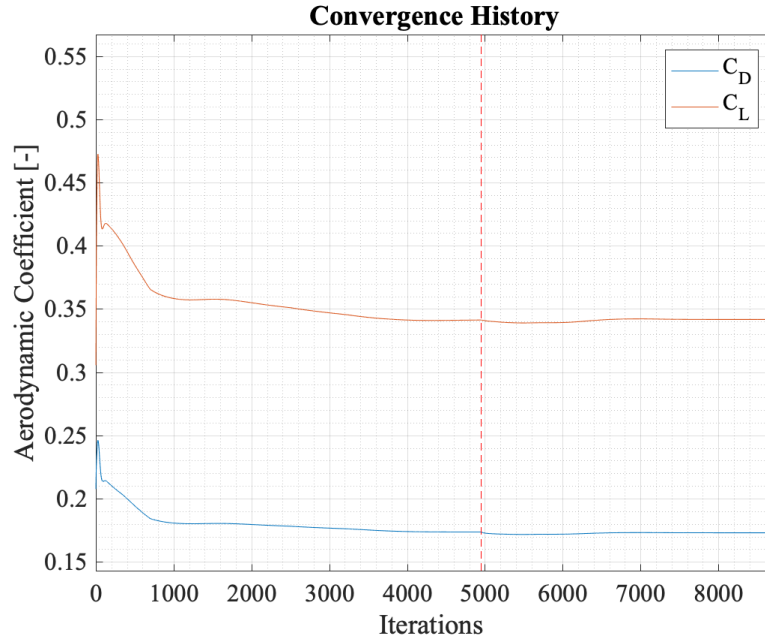


Figure 15: Convergence history with adaption for $\text{AoA} = 20^\circ$; red dashed-line indicates where iterations for the refined mesh began.

References

- [1] John D. Anderson. *Modern Compressible Flow with Historical Perspective*. McGraw Hill Education, 2003.
- [2] Rui Dilão and João Fonseca. Dynamic guidance of gliders in planetary atmospheres. *American Society of Civil Engineers*, 1(29), 1 2016.